

Coupling to real and virtual phonons in tunneling spectroscopy of superconductors

Jasmin Jandke,¹ Patrik Hlobil,² Michael Schackert,¹ Wulf Wulfhekel,¹ and Jörg Schmalian^{2,3}

¹*Physikalisches Institut, Karlsruher Institut für Technologie, 76131 Karlsruhe, Germany*

²*Institut für Theorie der Kondensierten Materie,
Karlsruher Institut für Technologie, 76131 Karlsruhe, Germany*

³*Institut für Festkörperphysik, Karlsruher Institut für Technologie, 76344 Karlsruhe, Germany*

(Dated: April 1, 2025)

Fine structures in the tunneling spectra of superconductors have been widely used to identify fingerprints of the interaction responsible for Cooper pairing. Here we show that for scanning tunneling microscopy (STM) of Pb, the inclusion of inelastic tunneling processes is crucial for the proper interpretation of these fine structures. For STM the usual McMillan inversion algorithm of tunneling spectra must therefore be modified to include inelastic tunneling events, an insight that is crucial for the identification of the pairing glue in conventional and unconventional superconductors alike.

PACS numbers: 74.55.+v, 74.81.Bd, 74.25.Jb, 74.25.Kc

Conventional superconductivity is caused by the attractive interaction between electrons near the Fermi energy mediated by phonons [1]. This leads to the formation of a gap 2Δ in the single particle density of states (DOS) of the electrons, and to quasi-particle peaks above the gap [2, 3]. Eliashberg extended the BCS theory to the limit of larger dimensionless electron-phonon coupling constants λ and included a realistic electron-phonon coupling and the detailed structure of the phonon spectrum [4]. As a consequence, the quasi-particle peaks near the Fermi surface are modified due to the interaction with phonons, leading to fine structures in the electronic DOS near the peaks of $\alpha^2F(\omega)$ shifted by Δ . The Eliashberg function $\alpha^2F(\omega)$ describes the phonon DOS, weighted by the electron-phonon coupling. Experimentally, these fine structures in the electronic DOS have been detected with electron tunneling spectroscopy on planar junctions [5–10]. In the pioneering work of McMillan and Rowell [11], the Eliashberg function could be reconstructed from the superconducting DOS by an inversion algorithm taking into account the interaction of electrons and virtual phonons. This method has been used to identify fingerprints of the phononic pairing glue in the electronic spectrum and thus to determine the pairing mechanism leading to superconductivity [12, 13]. It counts as a hallmark of condensed matter physics.

An alternative way to determine the Eliashberg function is to measure the energy dependence of the scattering of electrons with real phonons in the normal state using inelastic tunneling spectroscopy (ITS) [14–17]. This method is more direct, as the second derivative of the tunneling current I with respect to the bias voltage U is, under rather general assumptions, directly proportional to $\alpha^2F(\omega)$ [18]. Recently, this method has been combined with scanning tunneling microscopy (STM) to obtain local information on the Eliashberg function of Pb on a Cu(111) substrate [19].

In this work, we determine experimentally and ana-

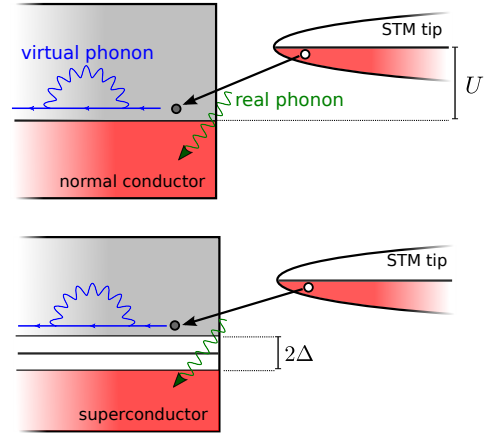


FIG. 1: Illustration of the inelastic tunneling processes in the normal and superconducting state. The inelastic tunneling process is accompanied by the excitation of real phonons (green). The renormalization of the electronic bandstructure via the exchange of virtual phonons (blue) has effects on both the elastic and the inelastic tunneling current.

lyze theoretically the tunneling conductance of Pb that is affected by the coupling to real phonons via inelastic tunneling and virtual phonons via many-body renormalizations. Comparing the two approaches to determine $\alpha^2F(\omega)$ on the same sample with the same tip of a low temperature STM, we show that interpreting tunneling spectra of superconductors via the McMillan inversion algorithm (and thus solely by its elastic contribution) can be an incomplete description. We demonstrate that inelastic contributions of the tunneling current can, in general, be of the order of the elastic contribution and show that we can understand experimental STM data from Pb tunneling in the normal and superconducting state, taking into account both elastic and inelastic tunneling processes. The combined analysis of elastic and inelastic tunneling processes is important to correctly identify fingerprints of the relevant interactions in the electronic

DOS and to identify the pairing glue for superconductivity. This is essential for conventional superconductors, such as Pb, but is expected to be even more important for unconventional pairing states, where an electronic pairing interaction is expected to fundamentally change its character upon entering the superconducting state.

The Hamiltonian $\mathcal{H} = \mathcal{H}_0 + \mathcal{H}_t$ of the combined substrate and tip consists of free electrons in the tip and electrons interacting with phonons in the substrate (we set $\hbar = 1$):

$$\begin{aligned} \mathcal{H}_0 = & \sum_{\mathbf{p},\sigma} \epsilon_{\mathbf{p}}^T c_{\mathbf{p},\sigma}^\dagger c_{\mathbf{p},\sigma} + \sum_{\mathbf{k},\sigma} \epsilon_{\mathbf{k}}^S c_{\mathbf{k},\sigma}^\dagger c_{\mathbf{k},\sigma} + \sum_{\mathbf{q},\mu} \omega_{\mathbf{q},\mu} a_{\mathbf{q},\mu}^\dagger a_{\mathbf{q},\mu} \\ & + \frac{1}{\sqrt{V_S}} \sum_{\substack{\mathbf{k},\mathbf{k}' \\ \sigma,\mu}} \alpha_{\mathbf{k}-\mathbf{k}',\mu} c_{\mathbf{k},\sigma}^\dagger c_{\mathbf{k}',\sigma} \phi_{\mathbf{k}-\mathbf{k}',\mu}. \end{aligned} \quad (1)$$

Here, $\phi_{\mathbf{q},\mu} = a_{\mathbf{q},\mu} + a_{-\mathbf{q},\mu}^\dagger$ is proportional to the lattice displacement, where $a_{\mathbf{q},\mu}$ is the phonon annihilation operator for momentum \mathbf{q} and phonon-branch μ and with dispersion $\omega_{\mathbf{q},\mu}$. $c_{\mathbf{k}/\mathbf{p},\sigma}^\dagger$ are the electron annihilation operators for the two subsystems: The tip (quasi-momentum \mathbf{p} , dispersion $\epsilon_{\mathbf{p}}^T$ and volume V_T) and the superconductor (quasi-momentum \mathbf{k} , dispersion $\epsilon_{\mathbf{k}}^S$ and volume V_S). For the latter we include the electron-phonon coupling $\alpha_{\mathbf{k}-\mathbf{k}',\mu}$ that gives rise to superconductivity. The electron-phonon interaction in the tip is assumed to be small. In addition, the tunneling part of the Hamiltonian includes elastic and inelastic tunneling processes[18, 20]:

$$\begin{aligned} \mathcal{H}_t = & \frac{1}{\sqrt{V_T V_S}} \sum_{\mathbf{k},\mathbf{p}} T_{\mathbf{k},\mathbf{p}} c_{\mathbf{k},\sigma}^\dagger c_{\mathbf{p},\sigma} + \text{h.c.}, \quad (2) \\ T_{\mathbf{k},\mathbf{p}} = & T_{\mathbf{k},\mathbf{p}}^e + \frac{1}{\sqrt{V_S}} \sum_{\mathbf{q},\mu} T_{\mathbf{k},\mathbf{p},\mathbf{q},\mu}^i \alpha_{\mathbf{q},\mu} \phi_{\mathbf{q},\mu} + \mathcal{O}(\phi_{\mathbf{q},\mu}^2). \end{aligned}$$

The first term of the tunneling amplitude $T_{\mathbf{k},\mathbf{p}}$ describes the elastic tunneling part, the second term corresponds to electron transitions via the emission/absorption of phonons, see Fig. 1. It is proportional to the bulk electron-phonon coupling $\alpha_{\mathbf{q},\mu}$ [18]. There can also be processes with a higher number of phonons, which will be discussed later.

In order to determine the tunneling current we employ the usual field theoretical methods (see Supplementary Material). While we derived results for arbitrary temperatures, here we concentrate on the regime where T is much smaller than all other energy scales of the system. We assume that the DOS of the tip is constant $\nu_T(\omega) \approx \nu_T^0$ and that the tunneling amplitudes are independent of momenta and phonon branches $T_{\mathbf{k},\mathbf{p}}^e = t^e$ and $T_{\mathbf{k},\mathbf{p},\mathbf{q},\mu}^i = t^i$. Then, to leading order in t^e , the second derivative of the elastic tunneling current with respect to the bias voltage

$$\frac{d^2 I^e}{dU^2} = -e\sigma_0 \tilde{\nu}'_S(-eU) \quad (3)$$

is proportional to the derivative of the normalized electron DOS $\tilde{\nu}_S(\omega) = \nu_S(\omega)/\nu_S^0$. ν_S^0 is the normal state DOS of the superconductor at the Fermi level. The conductance constant is given by $\sigma_0 = 4\pi e^2 |t^e|^2 \nu_T^0 \nu_S^0$. Eq.3 is the well known result of elastic tunneling [21–23]. In the normal state, $\tilde{\nu}_S(\omega)$ is essentially constant for small applied voltages and the second derivative of the elastic current vanishes. In the superconducting state, the opening of the superconducting gap and the excitation of virtual phonons lead to the mentioned fingerprints of superconductivity and the pairing glue in the elastic tunneling spectrum. Below we determine these structures from the solution of the nonlinear Eliashberg equations for given $\alpha^2 F(\omega)$.

The second derivative of the inelastic current due to the excitation of single real phonons is for $U > 0$ given by the convolution

$$\frac{d^2 I^i}{dU^2} = e\sigma_0 \frac{|t^i|^2}{|t^e|^2} \int_0^\infty d\omega \alpha^2 F'_{\text{tun}}(eU - \omega) \tilde{\nu}_S(-\omega). \quad (4)$$

The function $\alpha^2 F_{\text{tun}}(\omega) = \frac{1}{V_S} \sum_{\mathbf{q},\mu} |\alpha_{\mathbf{q},\mu}|^2 \delta(\omega - \omega_{\mathbf{q},\mu})$ is a weighted phonon DOS and is closely related, but not identical to the Eliashberg function $\alpha^2 F(\omega) = \frac{1}{V_S V} \sum_{\mathbf{k},\mathbf{k}',\mu} |\alpha_{\mathbf{k}-\mathbf{k}',\mu}|^2 \delta(\omega - \omega_{\mathbf{k}-\mathbf{k}',\mu}) \delta(\epsilon_{\mathbf{k}}^S) \delta(\epsilon_{\mathbf{k}'}^S)$. Both have similar features but can differ in fine-structure and amplitude. The result (4) is the generalization of the current in the normal state, where $\frac{d^2 I^i}{dU^2} \Big|_{\text{NC}} \sim \text{sign}(U) \alpha^2 F_{\text{tun}}(e|U|)$ is proportional to the weighted DOS of the phonons (or other collective excitations of the system), see Ref. [18, 20, 24, 25]. It was recently determined in STM measurements on Pb [19]. This normal state measurement allows for an estimate of the ratio $|t^i|^2/|t^e|^2$: the change in conductance from 0 to 10 meV is approximately $\frac{\sigma(10 \text{ meV}) - \sigma(0)}{\sigma(0)} \simeq 12\%$, where $\sigma(0) = \sigma_0$ is the (purely elastic) conductance at zero bias (see also Fig. 3a). Relating this to Eq. (3) and (4) in the normal state, one finds that $|t^i/t^e|^2 = 0.12 / \int_0^{10 \text{ meV}} d\omega \alpha^2 F_{\text{tun}}(\omega)$. Using this estimate and widely accepted Eliashberg functions for Pb [11] yields $|t^i/t^e|^2 \approx 30(\text{eV})^{-1}$ and elastic and inelastic contributions to the second derivative below T_c turn out to be comparable in magnitude, see Suppl. Material.

In the superconducting state, the inelastic contribution Eq.(4) has its major contribution for frequencies a bit below the energy of the phonon peaks shifted by the gap Δ . Since inelastic tunneling adds additional channels to the conductance, its contribution will have the opposite sign of the elastic contribution in (3) and can give pronounced positive peaks in the second derivative of the tunneling current followed by a negative peak of same amplitude. As we will see below, we find exactly these features in the tunneling current for the STM experiment on lead. Single phonon excitations are not the only contributions

to inelastic tunneling. Tunneling processes with a higher number of excited phonons will give similar terms as in (4) with higher convolutions of the Eliashberg-function such as $\alpha^4 F_{\text{tun}}^2(\omega) = \int d\omega' \alpha^2 F_{\text{tun}}(\omega - \omega') \alpha^2 F_{\text{tun}}(\omega')$ with other tunneling parameters. This amounts to replacing $\alpha^2 F_{\text{tun}}(\omega)$ in Eq. (4) by $\sum_{n=1} \kappa_n \alpha^{2n} F_{\text{tun}}^n(\omega)$, see Supplementary Material. The dimensionless coefficients κ_n determine the relative strength of higher order phonon excitations ($\kappa_1 = 1$).

After these qualitative considerations we present our experimental data for STM measurements on lead, followed by a detailed theoretical analysis. Measurements were performed with a home-build Joule-Thomson low-temperature STM (JT-STM)[26] at temperatures about 0.8 K. The JT-STM contains a magnet which allows to suppress superconductivity. In order to ensure that there is no significant inelastic signal of the tip at $|U| < 15$ mV, we use a chemically etched tungsten tip, known to have a weak electron-phonon coupling [27]. The n-type Si(111) crystals were carefully degassed at 700 °C for several hours and then flashed to 1150 °C for 30 seconds to remove the native oxide. Lead was evaporated at room temperature from a Knudsen cell with a deposition rate of 1.9 monolayers/min for 10 min. After deposition the samples were immediately transferred to the cryogenic STM. In agreement with previous studies [28–30], flat-top, wedge-like islands were observed (see Fig. 2), i.e. 3D islands appear on top of a wetting layer (WL). The islands are Pb single crystals with their $\langle 111 \rangle$ axis perpendicular to the substrate [29, 31, 32]. The first (second) derivative of the tunneling current dI/dU (d^2I/dU^2) of the islands was measured using a lock-in amplifier with a modulation voltage of $U_{\text{mod}} = 439 \mu\text{V}$.

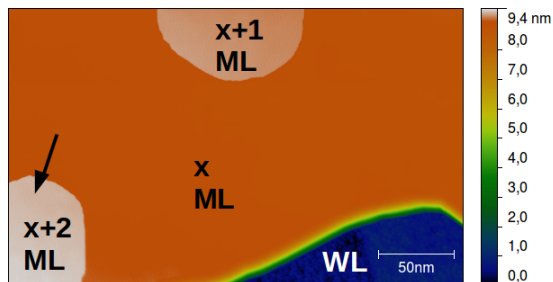


FIG. 2: STM topography of Pb on Si(111) ($300 \times 175 \text{ nm}^2$, 1 V, 1 nA). The thickness of the island was determined to $x \approx 30$ monolayers.

As a first measurement, we determine $\alpha^2 F_{\text{tun}}(\omega)$ of lead directly with ITS in the normal state. Pb islands were forced to the normal state by applying a magnetic field of 1 T normal to the sample plane. Since the elastic contribution vanishes in the normal state, the peaks of the second derivative of the current correspond to purely inelastic tunneling. Fig. 4 shows the measured $d^2I/dU^2 \sim \alpha^2 F_{\text{tun}}(eU)$ spectrum clearly revealing the

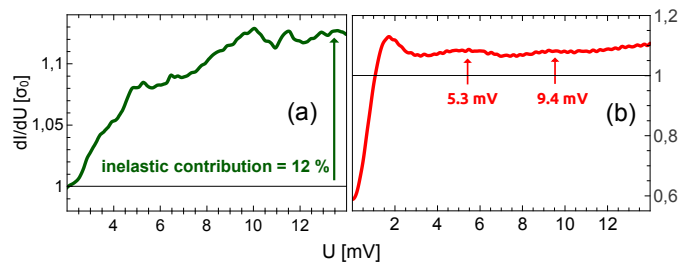


FIG. 3: Differential conductance dI/dU in the normal (a) and superconducting (b) state as a function of the bias voltage U measured on the island marked by arrow in Fig. 2. dI/dU in the normal state has been normalized to the low voltage conductance and the superconducting state was scaled with the same factor.

two characteristic phonon peaks that are also seen in the Eliashberg function $\alpha^2 F(\omega)$ determined by Ref. [11]. These peaks at $U \approx 4.05$ mV and $U \approx 8.3$ mV coincide with the energies of the “transversal” and “longitudinal” van Hove singularities in the phonon DOS of lead [33, 34]. The additional peak at $U \approx 12.5$ mV can be explained by tunneling processes via two-phonon emission. Note that also the second peak may already include such two-phonon processes.

Without magnetic field, the islands are in the superconducting state. As the local thickness of the islands (30 monolayers ≈ 10 nm) is smaller than the bulk coherence length of lead (83 nm [35]), the superconducting gap is not fully developed, see the conductance in Fig. 3b). This behavior has been seen before in Ref. [28, 29, 36–38]. Besides the Bogoliubov quasiparticle peak one clearly observes fine structures in the spectrum of the conductance around $U \approx 5.3$ mV and $U \approx 9.4$ mV. These energies correspond to the van Hove singularities in the phonon DOS $F(\omega)$ of lead shifted by the gap $\Delta \approx 1.2$ meV clearly indicating electron-phonon interaction induced effects. Furthermore, the typical $\omega/\sqrt{\omega^2 - \Delta^2}$ behavior in the BCS DOS is rapidly suppressed towards higher energies where the inelastic processes become important. This is in contrast to previous measurements on planar tunneling junctions of lead [5–10], but it can be understood by taking into account that the inelastic tunneling amplitude was about one order of magnitude smaller [15] than in our present experiment. Let us now investigate the second derivative of the tunneling current, which is significantly more sensitive to the fine structure induced by the electron-phonon interaction. As can be seen in Fig. 5, the measured positions of the peak-dip features around the zero axis correspond to the characteristic longitudinal and transversal phonon energies $\omega_{t/l}$ shifted by the gap $\Delta \approx 1.2$ meV. As was mentioned before, such symmetric peak-dip features in the superconducting state cannot be explained by purely elastic tunneling. However, taking into account the additional inelastic tunneling channels, we naturally can explain the finestructure of the tunnel-

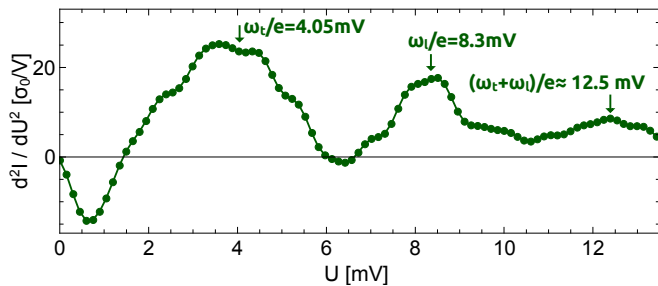


FIG. 4: Second derivative $d^2I/dU^2 \sim \alpha^2 F_{\text{tun}}(eU)$ measured in the normal conducting state ($T = 0.8$ K, $B = 1$ T).

ing current both in the normal *and* in the superconducting state.

For the theoretical fit, we first use a parameterization of the Eliashberg function obtained by McMillan and Rowell [11] to solve the Eliashberg equations numerically [39] and obtain the lead DOS $\nu_S(\omega)$ in the superconducting state. The elastic contribution to the second derivative is then easily calculated using Eq. (3). For the inelastic contribution we use the $\alpha^2 F_{\text{tun}}(\omega)$ function (without the negative dip at small voltages $U < 2$ mV that comes from a zero bias anomaly) and the already calculated DOS $\nu_S(\omega)$ to determine the convolution in Eq. (4), where the usage of the measured $\alpha^2 F_{\text{tun}}(\omega)$ function automatically includes two-phonon processes and yields the correct amplitude for the inelastic tunneling current. Finally, we convoluted our results with a Gaussian distribution (standard deviation $\sigma = 0.4$ meV), describing the experimental broadening due to temperature and the modulation voltage of the lock-in detection [17]. In Fig. 5 we compare the experimental data with the theoretical prediction of the elastic, inelastic and total contributions of the second derivative of the current. The elastic d^2I^e/dU^2 curve shows the typical dips around $\Delta + \omega_{t/1}$ predicted by the Eliashberg theory, whereas the total d^2I^{tot}/dU^2 also shows peaks of comparable height relative to the zero axis at slightly lower bias voltages (shifted down by the half-width $\gamma_{t/1}$ of the peaks in the phonon DOS). These symmetric peak-dip structures are also seen in the experimental data, such that we can understand the superconducting tunneling spectra taking into account the additional inelastic tunneling processes ($I^{\text{tot}} = I^e + I^i$) describing the excitation of real phonons.

Suppose, one would mistakenly assume that the total current only consists of an elastic contribution and attempt to identify the underlying interaction $\alpha^2 F(\omega)$ from a McMillan-Rowell analysis, one would of course not obtain the correct Eliashberg function.

In summary, we demonstrated experimentally and theoretically that in normal conducting Pb islands it is possible to directly measure the collective bosonic excitation spectrum, here phonons, using STM. In the normal conducting state, the obtained d^2I/dU^2 spectra is pro-

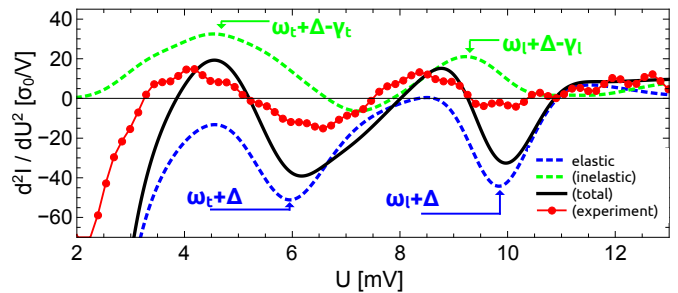


FIG. 5: Comparison of experimental data (red) and theoretical prediction in the superconducting state: Calculated elastic (blue), inelastic (green) and total (black) contribution to the second derivative of the tunneling current convoluted with a Gaussian function (standard deviation $\sigma = 0.4$ meV). Characteristic peak-dip features around the zero axis can only be explained taking into account elastic and inelastic channels ($I^{\text{tot}} = I^{\text{el}} + I^{\text{inel}}$).

portional to the weighted phonon DOS $\alpha^2 F_{\text{tun}}(\omega)$ and higher convolutions thereof. This is different in the superconducting state of Pb. Here, the obtained second derivative $d^2I/dU^2 = d^2I^e/dU^2 + d^2I^i/dU^2$ spectra are a composition of elastic and inelastic tunneling processes with fine structures in the same energy regime. Whereas the elastic part shows phonon features coming from self energy corrections (exchange of virtual phonons) in the DOS of the superconducting quasi-particles leading to dip features in the second derivative of the tunneling current, the inelastic part shows features of $\alpha^2 F_{\text{tun}}(\omega)$ shifted by the superconducting gap Δ giving rise to additional peak features of the same amplitude (excitation of real phonons). A rather unique signature of inelastic contributions are symmetric peak-dip features in d^2I/dU^2 around the zero axis. Those cannot be explained by only taking into account the elastic part d^2I^e/dU^2 . For this reason, the neglect of inelastic processes in STM experiments is in general not justified. Hence, when analyzing STM tunneling spectra via the McMillan inversion algorithm (purely elastic contribution) one should carefully subtract the inelastic contributions from the experimental tunneling current. Otherwise grossly incorrect conclusions about the pairing glue would be deduced from the tunneling spectrum.

Having found out experimentally and theoretically how the creation of real phonons and self energy correction in the quasiparticle DOS can be disentangled for conventional superconductors, the approach can be generalized to the investigation of corresponding bosonic structures in high temperature superconductors such as cuprates and iron pnictides for the future. A crucial difference to the phononic pairing glue is that in case of electronic pairing, the bosonic spectrum undergoes dramatic reorganization below T_c in form of a sharp resonance in the dynamic spin excitation spectrum [40–45]. Our results imply that great care must be taken in the proper inter-

pretation of the tunneling spectra of these systems and that real and virtual bosonic excitations must be disentangled in a fashion similar to our analysis for lead.

-
- [1] J. Bardeen, L. N. Cooper, and J. R. Schrieffer, *Phys. Rev.* **108**, 1175 (1957).
- [2] I. Giaever, *Phys. Rev. Lett.* **5**, 147 (1960).
- [3] J. Nicol, S. Shapiro, and P. H. Smith, *Phys. Rev. Lett.* **5**, 461 (1960).
- [4] G. M. Eliashberg, *Sov. Phys. JETP* **11**, 696 (1960).
- [5] I. Giaever, H. R. Hart, and K. Mergele, *Phys. Rev.* **126**, 941 (1962).
- [6] J. R. Schrieffer, D. J. Scalapino, and J. W. Wilkins, *Phys. Rev. Lett.* **10**, 336 (1963).
- [7] J. M. Rowell, A. G. Chynoweth, and J. C. Phillips, *Phys. Rev. Lett.* **9**, 59 (1962).
- [8] J. M. Rowell, P.W. Anderson, and D.E. Thomas, *Phys. Rev. Lett.* **10**, 334 (1963).
- [9] W. McMillan and J. Rowell, *Superconductivity Vol. 1*, ed. R. D. Parks (Dekker, New York, 1969) pp. 561-611.
- [10] I. Giaever, *Science* **183**, 1253 (1974).
- [11] W. L. McMillan and J. M. Rowell, *Phys. Rev. Lett.* **14**, 108 (1965).
- [12] D.J. Scalapino, J. W. Wilins, *Phys. Rev.* **148**, 263-279 (1966).
- [13] J.P. Carbotte, *Rev. Mod. Phys.* **62**, 1027 (1990).
- [14] A. Leger and J. Klein, *Phys. Lett.* **28A**, 751 (1969)..
- [15] J. M. Rowell, W. L. McMillan, and W. Feldmann, *Phys. Rev.* **180**, 658 (1969).
- [16] W. Wattamanuk, H. Kreuzer, and J. Adler, *Physics Letters A* **37**, 7 (1971).
- [17] J. Klein, A. Léger, M. Belin, D. Défourneau, and M. J. L. Sangster, *Phys. Rev. B* **7**, 2336 (1973).
- [18] M.E. Taylor, *Ultramicroscopy* **42**, 215 (1992).
- [19] M. Schackert et al., *Phys. Rev. Lett.* **114**, 047002 (2015).
- [20] Alan J. Bennett, C. B. Duke and S. D. Silverstein, *Phys. Rev.* **176**, 969 (1968).
- [21] J. Bardeen, *Phys. Rev. Lett.* **6**, 57 (1961).
- [22] M. H. Cohen, L. M. Falicov, and J. C. Phillips, *Phys. Rev. Lett.* **8**, 316 (1962).
- [23] Gerald D. Mahan, *Many-Particle Physics*, Springer, 3rd ed. (2000).
- [24] J. R. Kirtley and D. J. Scalapino, *Phys. Rev. Lett.* **65**, 798 (1990).
- [25] Ming-wen Xiao, Zheng-zhong Li, *Physica C: Superconductivity* **221**, 136 (1994).
- [26] L. Zhang, T. Miyamachi, T. Tomanić, R. Dehm, and W. Wulfhekel, *Rev. Sci. Instr.* **82**, 103702 (2011).
- [27] W. McMillan, *Phys. Rev.* **167**, 331 (1968).
- [28] C. Brun, I.-P. Hong, F. Patthey, I. Y. Sklyadneva, R. Heid, P. M. Echenique, K. P. Bohnen, E. V. Chulkov, and W.-D. Schneider, *Phys. Rev. Lett.* **102**, 207002, (2009).
- [29] D. Eom, S. Qin, M.-Y. Chou, and C. K. Shih, *Phys. Rev. Lett.* **96**, 027005 (2006).
- [30] I. B. Altfeder, K. A. Matveev, and D. M. Chen, *Phys. Rev.* **78**, 2815 (1997).
- [31] H. H. Weitering, D. R. Heslinga, and T. Hibam, *Phys. Rev. B* **45**, 5991 (1992).
- [32] M. Jalochowski, H. Knoppe, G. Lilienkamp and E. Bauer, *Phys. Rev. B* **46**, 4693 (1982).
- [33] R. Heid, K.-P. Bohnen, I. Yu. Skladneva, and E. V. Chulkov, *Phys. Rev. B* **81**, 174527 (2010).
- [34] B. N. Brockhouse, T. Arase, G. Caglioti, K. R. Rao, and A. D. B. Woods, *Phys. Rev.* **128**, 1099 (1962).
- [35] Charles Kittel, "Introduction to solid state physics", Wiley New York (2005).
- [36] T. Nishio, M. Ono, T. Eguchi, H. Sakata, and Y. Hasegawa, *Appl. Phys. Lett.* **88**, 113115 (2006).
- [37] T.Nishio, A. Nomura, K. Miyachi, T. Eguchi, H. Sakata, S. Lin, N. Hayashi, N. Nakai, M. Machida, and Y. Hasegawa, *Phys. Rev. Lett.* **101**, 167001 (2008).
- [38] S. Qin, J. Kim, Q. Niu, C-K. Shin, *Science* **324**, 1314 (2009).
- [39] J. Schmalian, M. Langer, S. Grabowski and K. H. Bennemann, *Computer Physics Communications* **93**, 141 (1996).
- [40] J. Rossat-Mignod, L. Regnault, C. Vettier, P. Bourges, P. Burllet, J. Bossy, J. Henry, and G. Lapertot, *Physica C* **86**, 185 (1991).
- [41] H. A. Mook, M. Yethiraj, G. Aeppli, T. E. Mason, and T. Armstrong, *Phys. Rev. Lett.* **70**, 3490 (1993).
- [42] H. Fong, P. Bourges, Y. Sidis, L. Regnault, A. Ivanov, G. Gu, N. Koshizuka, and B. Keimer, *Nature* **398**, 588 (1999).
- [43] A. D. Christianson, E. A. Goremychkin, R. Osborn, S. Rosenkranz, M. D. Lumsden, C. D. Malliakas, I. S. Todorov, H. Claus, D. Y. Chung, M. G. Kanatzidis, R. I. Bewley, and T. Guidi, *Nature* **456**, 930 (2008).
- [44] D.S. Inosov, P. B.J.T. Park, D.L. Sun, Y. Sidis, A. Schneidewind, K. Hradil, D. Haug, C.T. Lin, B. Keimer, and V. Hinkov, *Nat. Phys.* **6**, 178 (2010).
- [45] A. Abanov, A. Chubukov and J. Schmalian, *J. Electron Spectrosc. Relat. Phenom.* **117**, 129 (2001).

Supplementary Material to “Coupling to real and virtual phonons in the tunneling spectroscopy of superconductors”

DERIVATION OF THE TUNNEL CURRENT

Perturbative approach

The tunneling current is given by elementary charge times the change of the number of electrons $n_S = \sum_{k,\sigma} c_{k,\sigma}^\dagger c_{k,\sigma}$ in the superconductor

$$\begin{aligned} I &= -e \frac{d}{dt} \text{tr}[\rho(t)n_S] / \text{tr}[\rho(t)] \\ &= ie \text{tr}(\rho_0 [n_S(t), \mathcal{H}(t)]) / \text{tr}[\rho_0] \\ &= ie \langle [n_S(t), \mathcal{H}(t)] \rangle \end{aligned} \quad (5)$$

where $\rho(t) = U(t, \infty)\rho_0 U^\dagger(t, -\infty)$ is the time-dependent density matrix and $\langle \dots \rangle_0 = \langle \rho_0 \dots \rangle = \langle e^{-\beta\mathcal{H}} \dots \rangle$ is the expectation value of the system in thermal equilibrium with density matrix $\rho_0 = e^{-\beta\mathcal{H}}$. A suitable formalism to calculate the current (5) is the Keldysh Green function method (we follow the notation of Ref. [1]). The corresponding Keldysh action of the Hamiltonian (without bias voltage) employed in the main text of the paper is given by

$$\begin{aligned} S &= S_0 + S_t \\ S_0 &= \int_C dt \sum_{p,\sigma} \bar{c}_{p,\sigma}(t) (i\partial_t - \epsilon_p^T) c_{p,\sigma}(t) \\ &\quad + \int_C dt \sum_{k,\sigma} \bar{c}_{k,\sigma}(t) (i\partial_t - \epsilon_k^S) c_{k,\sigma}(t) \\ &\quad + \int_C dt \sum_{q,\mu} \bar{a}_{q,\mu}(t) (i\partial_t - \omega_{q,\mu}) a_{q,\mu}(t) \\ &\quad - \frac{1}{\sqrt{V_S}} \int_C dt \left[\sum_{\substack{k,k' \\ \sigma,\mu}} \alpha_{k-k',\mu} \bar{c}_{k,\sigma}(t) c_{k',\sigma}(t) \phi_{k-k',\mu}(t) + \text{h.c.} \right] \\ S_t &= -\frac{1}{\sqrt{V_S V_T}} \int_C dt \sum_{k,p} T_{k,p}^e \bar{c}_{k,\sigma}(t) c_{p,\sigma}(t) \\ &\quad - \frac{1}{V_S \sqrt{V_T}} \int_C dt \sum_{\substack{k,p,q \\ \sigma,\mu}} T_{k,p,q}^i \alpha_{q,\mu} \bar{c}_{k,\sigma}(t) c_{p,\sigma}(t) \phi_{q,\mu}(t) + \text{h.c.} \end{aligned} \quad (6)$$

where as usual we defined the phonon displacement field $\phi_{q,\mu} = a_{q,\mu} + a_{-q,\mu}^\dagger$ [3]. In order to derive the $I-U$ characteristic of the system we have to apply a finite voltage $eU = \mu_S - \mu_T$, which can be done easily by the substitution $c_{p,\sigma}(t) \rightarrow e^{-i\mu_T t} c_{p,\sigma}(t)$ and $c_{k,\sigma}(t) \rightarrow e^{-i\mu_S t} c_{k,\sigma}(t)$. The dispersion energies of the tip $\epsilon_p^T \rightarrow \xi_p^T = \epsilon_p^T - \mu_T$ and superconductor $\epsilon_k^S \rightarrow \xi_k^S = \epsilon_k^S - \mu_T$ are now measured relative to their chemical potentials and this leads to a time dependence of the tunneling matrix elements $T^e \rightarrow T^e e^{ieUt}$, $T^i \rightarrow T^i e^{ieUt}$ in the tunneling part S_t of the action.

We build up our perturbation theory by rewriting $\langle \dots \rangle = \int D[\bar{c}, c] D[\bar{a}, a] \dots e^{iS} = \langle e^{iS_t} \dots \rangle_0$

with the unperturbed expectation value $\langle \dots \rangle_0 = \int D[\bar{c}, c] D[\bar{a}, a] \dots e^{iS_0}$. The corresponding unperturbed propagators are then given in the R, A, K basis (also known as *Larkin-Ovchinnikov Representation*)

$$\begin{aligned} \hat{G}_{k/p}(t, t') &= -i \langle \left(\begin{array}{c} c_{k/p,\sigma}^1(t) \\ c_{k/p,\sigma}^2(t) \end{array} \right) \left(\begin{array}{c} c_{k/p,\sigma}^1(t') \\ c_{k/p,\sigma}^2(t') \end{array} \right)^\dagger \rangle_0 \\ &= \begin{pmatrix} G_{k/p}^R(t, t') & G_{k/p}^K(t, t') \\ 0 & G_{k/p}^A(t, t') \end{pmatrix} \\ \hat{D}_{q,\mu}(t, t') &= -i \langle \left(\begin{array}{c} \phi_{q,\mu}^{\text{cl}} \\ \phi_{q,\mu}^{\text{q}} \end{array} \right) \left(\begin{array}{c} \phi_{-q,\mu}^{\text{cl}} \\ \phi_{-q,\mu}^{\text{q}} \end{array} \right)^\dagger \rangle_0 \\ &= \begin{pmatrix} D_{q,\mu}^K(t, t') & D_{q,\mu}^R(t, t') \\ D_{q,\mu}^A(t, t') & 0 \end{pmatrix} \end{aligned} \quad (7)$$

where the retarded propagators are given in energy representation $f(\omega) = \int_{-\infty}^{\infty} dt f(t) e^{i\omega t}$ as

$$\begin{aligned} G_k^R(\omega) &= \rightarrow = \frac{Z_k^R(\omega) \omega + \xi_k^S}{[Z_k^R(\omega) \omega]^2 - [\xi_k^S]^2 - \Phi_k^R(\omega)^2} \\ F_k^R(\omega) &= \rightarrow \leftarrow = \frac{-\Phi_k^R(\omega)}{[Z_k^R(\omega) \omega]^2 - [\xi_k^S]^2 - \Phi_k^R(\omega)^2} \\ G_p^R(\omega) &= - \rightarrow - = \frac{1}{\omega - \xi_p^S + i0} \\ D_{q,\mu}^R(\omega) &= \sim \sim \sim = \frac{2\omega_{q,\mu}}{(\omega + i0)^2 - \omega_{q,\mu}^2} \end{aligned} \quad (8)$$

For the superconductor, we use the known framework of Eliashberg theory. Therefore, $Z_k^R = 1 - \frac{\Sigma_k^R(\omega) - \Sigma_k^A(-\omega)}{2\omega}$ is the renormalization function of the lead superconductor S and $\Sigma_k^{R/A}(\omega) = \Sigma_k(\omega \pm i0)$ is the phonon-induced normal self-energy, see Fig. 6. We neglected the correction of the pure dispersion ξ_k^S due to the coupling to the phonons, because it will basically just give an unimportant shift of the chemical potential and can be assumed to be incorporated in the electronic dispersion already from the beginning. The anomalous self-energy $\Phi_k^R(\omega) = \Phi_k(\omega + i0)$ is depicted in Fig. 6 and we also gave the expression for the anomalous propagator $F_k^R(\omega)$, even though we will only need the normal particle propagator (since in the NIS-junction there is no Josephson effect). We neglect the renormalization of the phonon spectrum due to the interaction with the electrons, which could be incorporated easily by a phonon self-energy that would just lead to a small broadening and modification of the phonon spectral weight. Since we consider the sub-systems S and T to be in thermal equilibrium, the Keldysh propagators have the simple structure

$$\begin{aligned} G_{k/p}^K(\omega) &= [1 - 2n_F(\omega)] \underbrace{[G_{k/p}^R(\omega) - G_{k/p}^A(\omega)]}_{-2\pi i A_{k/p}(\omega)}, \\ D_{q,\mu}^K(\omega) &= [1 + 2n_B(\omega)] \underbrace{[D_{q,\mu}^R(\omega) - D_{q,\mu}^A(\omega)]}_{-2\pi i [A_{q,\mu}(\omega) - A_{q,\mu}(-\omega)]}, \end{aligned} \quad (9)$$

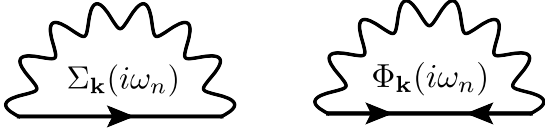


FIG. 6: Normal and anomalous self-energy that appear in the Eliashberg-theory.

where $n_F(\omega)$ is the Fermi and $n_B(\omega)$ the Bose function with temperature T and we defined the spectral weights $A_{\mathbf{k}/\mathbf{p}}(\omega)$, $A_{\mathbf{q},\mu}(\omega)$ of the electron and phonon systems. In our case $A_{\mathbf{q},\mu}(\omega) = \delta(\omega - \omega_{\mathbf{q},\mu})$. For completeness, we also give the explicit expressions for the greater/lesser Green functions

$$G_{\mathbf{k}/\mathbf{p}}^{>/<}(\omega) = -2\pi i \begin{Bmatrix} 1 - n_F(\omega) \\ -n_F(\omega) \end{Bmatrix} A_{\mathbf{k}/\mathbf{p}}(\omega) \quad (10)$$

$$D_{\mathbf{q},\mu}^{>/<}(\omega) = -2\pi i \begin{Bmatrix} 1 + n_B(\omega) \\ n_B(\omega) \end{Bmatrix} \left[A_{\mathbf{q},\mu}(\omega) - A_{\mathbf{q},\mu}(-\omega) \right]$$

Following Eq. (5) it is easy to determine the explicit expression for the current

$$\begin{aligned} I &= ie \langle \sum_{\mathbf{k},\mathbf{p}} \begin{pmatrix} c_{\mathbf{p},\sigma}^-(t) \\ c_{\mathbf{k},\sigma}^-(t) \end{pmatrix}^\dagger \begin{pmatrix} 0 & -[T_{\mathbf{k},\mathbf{p}}^+(t)]^* \\ T_{\mathbf{k},\mathbf{p}}^-(t) & 0 \end{pmatrix} \begin{pmatrix} c_{\mathbf{p},\sigma}^+(t) \\ c_{\mathbf{k},\sigma}^+(t) \end{pmatrix} \rangle \\ &= ie \langle \sum_{\mathbf{k},\mathbf{p}} \begin{pmatrix} c_{\mathbf{p},\sigma}^-(t) \\ c_{\mathbf{k},\sigma}^-(t) \end{pmatrix}^\dagger \begin{pmatrix} 0 & -[T_{\mathbf{k},\mathbf{p}}^+(t)]^* \\ T_{\mathbf{k},\mathbf{p}}^-(t) & 0 \end{pmatrix} \begin{pmatrix} c_{\mathbf{p},\sigma}^+(t) \\ c_{\mathbf{k},\sigma}^+(t) \end{pmatrix} e^{iS_t} \rangle_0 \\ &\approx -e \langle \sum_{\mathbf{k},\mathbf{p}} \begin{pmatrix} c_{\mathbf{p},\sigma}^-(t) \\ c_{\mathbf{k},\sigma}^-(t) \end{pmatrix}^\dagger \begin{pmatrix} 0 & -[T_{\mathbf{k},\mathbf{p}}^+(t)]^* \\ T_{\mathbf{k},\mathbf{p}}^-(t) & 0 \end{pmatrix} \begin{pmatrix} c_{\mathbf{p},\sigma}^+(t) \\ c_{\mathbf{k},\sigma}^+(t) \end{pmatrix} S_t \rangle_0 \end{aligned} \quad (11)$$

where we defined the total tunneling matrix element $T_{\mathbf{k},\mathbf{p}}^\pm(t) = e^{ieUt} [T_{\mathbf{k},\mathbf{p}}^e + \sum_{\mathbf{q},\mu} T_{\mathbf{k},\mathbf{p}}^e \alpha_{\mathbf{q},\mu} \phi_{\mathbf{q},\mu}^\pm(t)]$ (with phonon field ϕ^\pm on the upper/lower Keldysh contour) and in the end expanded in leading order of $T_{\mathbf{k},\mathbf{p}}$. Also, we defined the creation operators to be defined on the lower Keldysh contour (index $-$) and the annihilation operators on the upper Keldysh contour (index $+$), since the electron first has to leave one side before it can tunnel through the barrier to the other side. This time ordering can be conveniently expressed in Keldysh theory and we also assumed the phonons (field ϕ^\pm) to be excited/absorbed on the same contour as the electrons on the superconductor S . The tunneling action can be written in a similar way as

$$\begin{aligned} S_t &= - \int_C dt \sum_{\mathbf{k},\mathbf{p}} \begin{pmatrix} c_{\mathbf{p},\sigma}(t) \\ c_{\mathbf{k},\sigma}(t) \end{pmatrix}^\dagger \begin{pmatrix} 0 & [T_{\mathbf{k},\mathbf{p}}(t)]^* \\ T_{\mathbf{k},\mathbf{p}}(t) & 0 \end{pmatrix} \begin{pmatrix} c_{\mathbf{p},\sigma}(t) \\ c_{\mathbf{k},\sigma}(t) \end{pmatrix} \\ &= - \int_{-\infty}^{\infty} dt \sum_{\mathbf{k},\mathbf{p}} \sum_{\alpha=\pm} \alpha \begin{pmatrix} c_{\mathbf{p},\sigma}^\alpha(t) \\ c_{\mathbf{k},\sigma}^\alpha(t) \end{pmatrix}^\dagger \begin{pmatrix} 0 & [T_{\mathbf{k},\mathbf{p}}^\alpha(t)]^* \\ T_{\mathbf{k},\mathbf{p}}^\alpha(t) & 0 \end{pmatrix} \begin{pmatrix} c_{\mathbf{p},\sigma}^\alpha(t) \\ c_{\mathbf{k},\sigma}^\alpha(t) \end{pmatrix} \end{aligned} \quad (12)$$

Elastic current

Performing the contractions in Eq. (11) we find the elastic current

$$\begin{aligned} I^e &= 2e \int_{-\infty}^{\infty} d\tau \frac{1}{V_S V_T} \sum_{\mathbf{k},\mathbf{p}} |T_{\mathbf{k},\mathbf{p}}^e|^2 e^{ieU\tau} \sum_{\alpha=\pm} \alpha \\ &\quad [G_{\mathbf{k}}^{\alpha,-}(-\tau) G_{\mathbf{p}}^{+, \alpha}(\tau) - G_{\mathbf{k}}^{+, \alpha}(-\tau) G_{\mathbf{p}}^{\alpha,-}(\tau)] \\ &= -4e \int_{-\infty}^{\infty} d\tau \frac{1}{V_S V_T} \sum_{\mathbf{k},\mathbf{p}} |T_{\mathbf{k},\mathbf{p}}^e|^2 e^{ieU\tau} \\ &\quad [\text{Im} G_{\mathbf{k}}^<(-\tau) \text{Im} G_{\mathbf{p}}^R(\tau) - \text{Im} G_{\mathbf{k}}^R(-\tau) \text{Im} G_{\mathbf{p}}^<(\tau)] \end{aligned} \quad (13)$$

where we used the definition of the greater/lesser $G^{>/<}$ and time-ordered/anti-time-ordered Green function $G^{T/\bar{T}}$, see Section of the Supplementary Material. In the end, we used the known identities that relate $G^{T/\bar{T}}$ to the greater, lesser, retarded and advanced propagators. In Fig. 7 we show the corresponding Feynman diagram for the elastic tunneling current for the leading order in the tunneling element. After transforming to Fourier space and inserting the explicit expressions of the propagators in thermal equilibrium, we find

$$\begin{aligned} I^e &= 4\pi e \int_{-\infty}^{\infty} d\omega \frac{1}{V_S V_T} \sum_{\mathbf{k},\mathbf{p}} |T_{\mathbf{k},\mathbf{p}}^e|^2 \\ &\quad [n_F(\omega) - n_F(\omega + eU)] A_{\mathbf{k}}(\omega) A_{\mathbf{p}}(\omega + eU), \end{aligned} \quad (14)$$

which is the usual expression for the elastic current in the Landauer-Büttlinger transport theory assuming perfect quasiparticles $A_{\mathbf{k}/\mathbf{p}}(\omega) = \delta(\omega - \epsilon_{\mathbf{k}/\mathbf{p}}^{S/T})$.

The elastic conductance $G^e(U) = \frac{dI^e}{dU}$ will now be calculated using the usual approximation $T_{\mathbf{k},\mathbf{p}}^e = t^e = \text{const.}$ for small voltages $U \ll E_F \sim 1 \text{ eV}$ and small temperatures ($T \ll E_F$ in the normal conductor or $T \ll \Delta$ in the superconductor with gap Δ), such that $n_F(\epsilon) \approx \theta(-\epsilon)$. Assuming the DOS of the tip system $\nu^T(\omega) = 1/V_T \sum_{\mathbf{p}} A_{\mathbf{p}}(\omega) \approx \nu_T^0$ to be constant near the Fermi surface, we can then rewrite the elastic current (14) to be

$$I^e = 4\pi \nu_T^0 e |t^e|^2 \int_{-eU}^0 d\omega \nu^S(\omega), \quad (15)$$

where we defined as usual the DOS of the superconductor as $\nu(\omega) = 1/V_S \sum_{\mathbf{k}} A_{\mathbf{k}}(\omega)$. As it is well known, the elastic conductance is the first derivative of the current with respect to the bias voltage U

$$\frac{dI^e}{dU} = 4\pi \nu_T^0 e^2 |t^e|^2 \nu(-eU) = \sigma_0 \tilde{\nu}(-eU) \quad (16)$$

is then proportional to the normalized DOS $\tilde{\nu}(\omega) = \nu(\omega)/\nu_S^0$ of the superconductor. Here, we defined ν_S^0 as

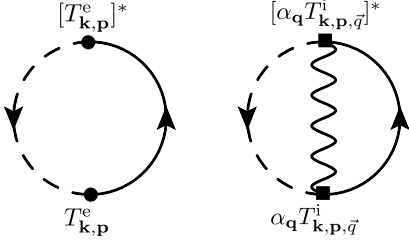


FIG. 7: Feynman diagrams for the elastic (left) and inelastic (right) tunneling current in leading order T^e, T^i .

the DOS and $\sigma_0 = 4\pi\nu_T^0\nu_S^0e^2|t^e|^2$ as the elastic conductance in the normal state. The corresponding second derivative of the elastic current is then given by

$$\frac{d^2 I^e}{dU^2}(U) = -e\sigma_0\nu'(-eU). \quad (17)$$

Inelastic current

The inelastic current can similarly be expressed by performing the contractions of (11) containing the phonon-

$$I^i = -4\pi e \int d\omega_1 d\omega_2 \frac{1}{V_S^2 V_T} \sum_{k,p,q} |T_{k,p,q,\mu}^i \alpha_{q,\mu}|^2 \left[A_{q,\mu}(\omega_1) A_k(\omega_2) A_p(\omega_2 - \omega_1 + eU) \left(n_F(\omega_2 - \omega_1 + eU) n_B(\omega_1) [1 - n_F(\omega_2)] - n_F(\omega_2) [1 + n_B(\omega_1)] [1 - n_F(\omega_2 - \omega_1 + eU)] \right) + A_{q,\mu}(\omega_1) A_k(\omega_2) A_p(\omega_2 + \omega_1 + eU) \left(n_F(\omega_2 + \omega_1 + eU) [1 + n_B(\omega_1)] [1 - n_F(\omega_2)] - n_F(\omega_2) n_B(\omega_1) [1 - n_F(\omega_2 + \omega_1 + eU)] \right) \right] \quad (19)$$

The first/third term describes the tunneling of an electron from the tip to the superconductor via the absorption/excitation of a phonon and the second/fourth term the tunneling from the superconductor to the tip via a phonon excitation/absorption, see also Fig. 8. As in the elastic case, we apply the following simplifications: A constant inelastic vertex $T_{k,p,q,\mu}^i = t^i$ and a constant DOS of the tip. Let us define the weighted DOS of the phonons in the superconductor as

$$\begin{aligned} \alpha^2 F_{\text{tun}}(\omega) &= \frac{1}{V_S} \sum_{q,\mu} |\alpha_{q,\mu}|^2 A_{q,\mu}(\omega) \\ &= \frac{1}{V_S} \sum_{q,\mu} |\alpha_{q,\mu}|^2 \delta(\omega - \omega_{q,\mu}), \end{aligned} \quad (20)$$

which is very similar to the Eliashberg function besides a different momentum average. For low temperature $k_B T \ll \omega_D, E_F$ only the processes that excite a phonon

fields and expressing the occurring propagators in terms of retarded, advanced, greater and lesser propagators

$$\begin{aligned} I^i &= 2ie \int_{-\infty}^{\infty} d\tau \frac{1}{V_S^2 V_T} \sum_{k,p,q,\mu} |T_{k,p,q,\mu}^i \alpha_{q,\mu}|^2 e^{ieU\tau} \sum_{\alpha=\pm} \alpha \\ &\quad \left[G_{\mathbf{k}}^{\alpha,-}(-\tau) G_{\mathbf{p}}^{+,\alpha}(\tau) D_{\mathbf{q},\mu}^{-,\alpha}(\tau) - G_{\mathbf{k}}^{+,\alpha}(-\tau) G_{\mathbf{p}}^{\alpha,-}(\tau) D_{\mathbf{q},\mu}^{\alpha,+}(\tau) \right] \\ &= 4e \int_{-\infty}^{\infty} d\tau \frac{1}{V_S^2 V_T} \sum_{k,p,q,\mu} |T_{k,p,q,\mu}^i \alpha_{q,\mu}|^2 e^{ieU\tau} \\ &\quad \left[\text{Im} G_{\mathbf{k}}^<(-\tau) \text{Im} G_{\mathbf{p}}^<(\tau) \text{Im} D_{\mathbf{q},\mu}^R(\tau) + \text{Im} G_{\mathbf{k}}^<(-\tau) \text{Im} G_{\mathbf{p}}^R(\tau) \text{Im} D_{\mathbf{q},\mu}^>(\tau) - \text{Im} G_{\mathbf{k}}^R(-\tau) \text{Im} G_{\mathbf{p}}^<(\tau) \text{Im} D_{\mathbf{q},\mu}^<(\tau) \right] \quad (18) \end{aligned}$$

After going to Fourier space and inserting the corresponding electron and phonon propagators defined in Sec. , we can finally rewrite the inelastic current as

lead to an inelastic contribution to the tunneling current since there are no phonons in the system and the Fermi function can be approximated as a step function $n_F(\omega) = \theta(-\omega)$. We then find

$$I^i = 4\pi e \nu_T^0 |t^i|^2 \int d\omega_1 d\omega_2 \alpha^2 F_{\text{tun}}(\omega_1) \nu^S(\omega_2) \left[\theta(-\omega_2) \theta(-\omega_1 + \omega_2 + eU) - \{\omega_2, U \rightarrow -\omega_2, -U\} \right] \quad (21)$$

For particle-hole symmetric electronic systems, we can directly write down the corresponding expression for the first and second derivative of the inelastic current as

$$\begin{aligned} \frac{dI^i}{dU} &= \sigma_0 \left| \frac{t^i}{t^e} \right|^2 \int_0^{\infty} d\omega \alpha^2 F_{\text{tun}}(e|U| - \omega) \tilde{\nu}^S(\omega) \\ \frac{d^2 I^i}{dU^2} &= e\sigma_0 \left| \frac{t^i}{t^e} \right|^2 \text{sign}(U) \int_0^{\infty} d\omega \alpha^2 F'_{\text{tun}}(e|U| - \omega) \tilde{\nu}^S(-\omega) \end{aligned} \quad (22)$$

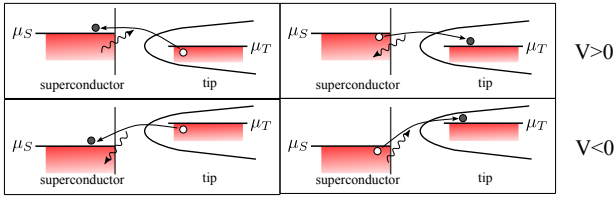


FIG. 8: Inelastic tunneling processes for $V > 0$ and $V < 0$ via the emission/absorption of phonons.

Multiple phonon processes

If we consider tunneling processes with a higher number of excited phonons we can formally write down the

following tunneling processes

$$\delta H_t^{(n)} = \frac{1}{\sqrt{V_t} V_S^{\frac{n+1}{2}}} \sum_{\substack{k,p,q_1,\dots,q_n \\ \sigma,\mu_1,\dots,\mu_n}} T_{k,p,q_1,\dots,q_n,\mu_1,\dots,\mu_n}^i \alpha_{q_1,\mu_1} \dots \alpha_{q_n,\mu_n} c_{k,\sigma}^\dagger c_{p,\sigma} \phi_{q_1,\mu_1} \dots \phi_{q_n,\mu_n} \quad (23)$$

In the low temperature limit $k_B T \ll \omega_D, E_F$, it is then straightforward to generalize the result (21) to the n-phonon process (demanding energy conservation and Fermi statistic for the leads)

$$I^{i,(n)} = 4\pi e \nu_T^0 \left| t^{i,(n)} \right|^2 \int d\omega_1 \dots d\omega_n d\omega_{n+1} \alpha^2 F_{\text{tun}}(\omega_1) \dots \alpha^2 F_{\text{tun}}(\omega_n) \nu^S(\omega_{n+1}) \left[\theta(-\omega_{n+1}) \theta(\omega_{n+1} - \omega_n - \dots - \omega_1 + eU) - \{ \omega_{n+1}, U \rightarrow -\omega_{n+1}, -U \} \right] \quad (24)$$

For the conductance, we then find for particle-hole symmetric systems

$$\begin{aligned} \frac{dI^{i,(n)}}{dU} &= \sigma_0 \left| \frac{t^{i,(n)}}{t^e} \right|^2 \text{sign}(U) \int_0^\infty d\omega d\omega_1 \dots d\omega_{n-1} \alpha^2 F_{\text{tun}}(e|U| - \omega - \omega_1) \alpha^2 F_{\text{tun}}(\omega_1 - \omega_2) \dots \alpha^2 F_{\text{tun}}(\omega_{n-2} - \omega_{n-1}) \tilde{\nu}_S(\omega) \\ &= \sigma_0 \left| \frac{t^{i,(n)}}{t^e} \right|^2 \text{sign}(U) \int_0^\infty d\omega \alpha^{2n} F_{\text{tun}}^n(e|U| - \omega) \tilde{\nu}_S(\omega) \end{aligned} \quad (25)$$

where we defined the convolution

$$\alpha^{2n} F_{\text{tun}}^n(\omega) = \int_0^\infty d\omega_1 \dots d\omega_{n-1} \alpha^2 F_{\text{tun}}(\omega - \omega_1) \alpha^2 F_{\text{tun}}(\omega_1 - \omega_2) \dots \alpha^2 F_{\text{tun}}(\omega_{n-2} - \omega_{n-1}) \quad (26)$$

ELASTIC AND INELASTIC STM TUNNELING FOR SINGLE MODE

In order to get a qualitative understanding of the inelastic tunneling contribution in the superconducting state, let us analyze a simple toy model. The toy model consists of a single phonon mode with $\alpha^2 F_{\text{tun}}(\omega) \simeq \alpha^2 F(\omega) = A_0 f(\omega) \frac{\gamma_0}{(\omega - \omega_0)^2 + \gamma_0^2}$ with characteristic phonon energy $\omega_0 = 5$ meV and half-width γ_0 . The function $f(\omega) = \frac{\omega^2}{\omega^2 + (1 \text{ meV})^2}$ ensures the proper low frequency behavior of acoustic phonons and rapidly approaches unity for larger frequencies. The value A_0 is chosen such that the dimensionless electron-phonon coupling constant $\lambda = 2 \int_0^\infty d\omega \alpha^2 F(\omega) / \omega = 1.5$. We use $\mu^* = 0.1$ for the pseudopotential, such that solving the Eliashberg equations yields a gap value $\Delta \simeq 1$ meV. In Fig. 9 we see the resulting second derivative of the tunneling current, which is more sensitive to the fine-structure than the con-

ductance, for the above mentioned elastic and inelastic tunneling for different peak width γ_0 in the superconducting state. As was seen in the experiments we use the ratio $|t^i/t^e|^2 \approx 0.12 / \int_0^{10 \text{ meV}} d\omega \alpha^2 F(\omega)$. The inelastic contribution Eq. (22) has its major contribution for frequencies a bit below the energy of the phonon peaks shifted by the gap Δ . Since inelastic tunneling adds additional channels to the conductance, its contribution will have the opposite sign of the elastic contribution in (17) and can give pronounced positive peaks in the second derivative of the tunneling current followed by a negative peak of same amplitude. These symmetric peak-dip features around the zero axis in the second derivative of the tunneling current are characteristic for the joint elastic and inelastic STM. In the present example, we were not able to find an Eliashberg function that would yield such a tunneling spectra from the purely elastic tunneling contribution Eq. (17). Even for very sharp Eliashberg

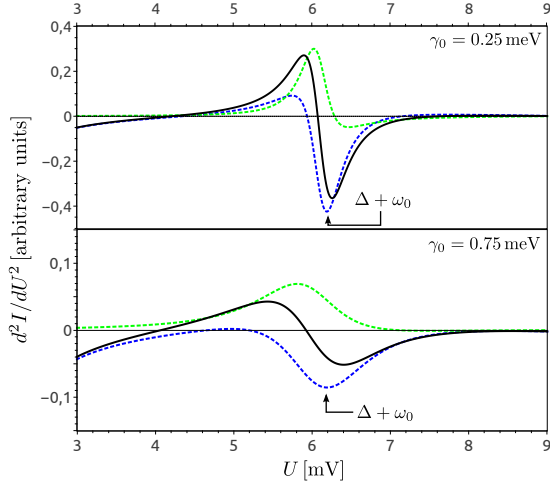


FIG. 9: Elastic (blue dashed), inelastic (green dashed) contribution to the total (black solid) second derivative of the current d^2I/dU^2 in the superconducting state for different peak width γ_0 . The additional inelastic contribution will lead to a peak-dip feature with similar positive and negative amplitude in the second derivative, whereas the purely elastic contribution only pronounces the dip at the shifted phonon frequency $eU \approx \Delta + \omega_0$ strongly.

spectra where the second derivative of the tunneling current can be clearly positive for some voltages, see upper picture in Fig. 9, the following dip will always be much more pronounced if one only considers the elastic tunneling contribution.

IMPORTANT RELATIONS OF NON-EQUILIBRIUM PROPAGATORS

Following Ref. [1] we define for both the fermionic and the bosonic fields $\phi(t)$ the greater, lesser, time-ordered and anti-time-ordered Green's functions as

$$\begin{aligned}
 G^<(t, t') &= G^{+-}(t, t') = -i\langle \phi^+(t)\bar{\phi}^-(t') \rangle \\
 G^>(t, t') &= G^{-+}(t, t') = -i\langle \bar{\phi}^-(t)\phi^+(t') \rangle \\
 G^{\mathcal{T}}(t, t') &= G^{++}(t, t') = -i\langle \phi^+(t)\bar{\phi}^+(t') \rangle \\
 G^{\bar{\mathcal{T}}}(t, t') &= G^{--}(t, t') = -i\langle \bar{\phi}^-(t)\bar{\phi}^-(t') \rangle
 \end{aligned}
 \tag{27}$$

We can now perform the Keldysh rotation to the classical and quantum fields in the bosonic case:

$$\begin{aligned}
 \phi^{\text{cl}}(t) &= \frac{1}{\sqrt{2}}[\phi^+(t) + \phi^-(t)] \\
 \phi^{\text{q}}(t) &= \frac{1}{\sqrt{2}}[\phi^+(t) - \phi^-(t)]
 \end{aligned}
 \tag{28}$$

and similar for the conjugate fields $\bar{\phi}(t)$. However, for the fermionic fields we use the Ovchinnikov-Larkin convention [2]

$$\begin{aligned}
 \phi^1(t) &= \frac{1}{\sqrt{2}}[\phi^+(t) + \phi^-(t)] \\
 \phi^2(t) &= \frac{1}{\sqrt{2}}[\phi^+(t) - \phi^-(t)] \\
 \bar{\phi}^1(t) &= \frac{1}{\sqrt{2}}[\bar{\phi}^+(t) - \bar{\phi}^-(t)] \\
 \bar{\phi}^2(t) &= \frac{1}{\sqrt{2}}[\bar{\phi}^+(t) + \bar{\phi}^-(t)]
 \end{aligned}
 \tag{29}$$

For the fermionic and bosonic cases, the retarded, advanced and Keldysh propagators are then defined as in Eq. (7). The relations between the different Green's functions ($>$, $<$, \mathcal{T} , $\bar{\mathcal{T}}$, R , A , K) can be summarized by

$$\begin{aligned}
 0 &= G^{\mathcal{T}} + G^{\bar{\mathcal{T}}} - G^> - G^< \\
 G^K &= G^> + G^< \\
 G^R &= \frac{1}{2}[G^{\mathcal{T}} - G^{\bar{\mathcal{T}}} + G^> - G^<] \\
 G^A &= \frac{1}{2}[G^{\mathcal{T}} - G^{\bar{\mathcal{T}}} - G^> + G^<]
 \end{aligned}
 \tag{30}$$

-
- [1] A. Kamenev, Field theory of non-equilibrium systems, Cambridge Univ. Press (2011)
 [2] A. I. Larkin and Y. N. Ovchinnikov, Sov. Phys. JETP **41**, 960 (1975)
 [3] which is often defined with an additional factor $1/\sqrt{2}$